arXiv:1610.02864v1 [q-bio.PE] 10 Oct 2016

Evolution of new regulatory functions on biophysically realistic fitness landscapes

Tamar Friedlander*, Roshan Prizak*, Nicholas H. Barton,

Gašper Tkačik

* T.F. and R.P. contributed equally to this work.

Institute of Science and Technology Austria, Am Campus 1, A-3400

Klosterneuburg, Austria

October 11, 2016

Abstract

Regulatory networks consist of interacting molecules with a high degree of mutual chemical specificity. How can these molecules evolve when their function depends on maintenance of interactions with cognate partners and simultaneous avoidance of deleterious "crosstalk" with noncognate molecules? Although physical models of molecular interactions provide a framework in which co-evolution of network components can be analyzed, most theoretical studies have focused on the evolution of individual alleles, neglecting the network. In contrast, we study the elementary step in the evolution of gene regulatory networks: duplication of a transcription factor followed by selection for TFs to specialize their inputs as well as the regulation of their downstream genes. We show how to coarse grain the complete, biophysically realistic genotype-phenotype map for this process into macroscopic functional outcomes and quantify the probability of attaining each. We determine which evolutionary and biophysical parameters bias evolutionary trajectories towards fast emergence of new functions and show that this can be greatly facilitated by the availability of "promiscuity-promoting" mutations that affect TF specificity.

Introduction

Phenotypes evolve largely through changes in gene regulation [1, 2, 3, 4], and such evolution may be flexible and rapid [5, 6]. Of particular importance are mutations affecting affinity and specificity of transcription factors (TFs) for their upstream signals or for their binding sites, short fragments of DNA that TFs interact with to activate or repress transcription of specific target genes. Mutations in these binding sites or at sites that alter TF specificity are crucial because of their ability to "rewire" the regulatory network—to weaken or completely remove existing interactions and add new ones, either functional or spurious. Emergence of novel functions in such a network will usually be constrained to evolutionary trajectories that maintain a viable pattern of existing interactions. This raises a fundamental question about the effects of such constraints on the accessibility of different regulatory architectures and the timescales needed to reach them.

The case that we focus on here is the divergence of gene regulation, which can give rise to a variety of new phenotypes, e.g., via expansion in TF families. A regulatory function previously accomplished by a single (or several) TF(s) is now carried out by a larger number of TFs, allowing for additional fine-tuning and precision, or, alternatively, for an expansion of the regulatory scope [7, 8, 9, 10, 11, 12, 13, 14, 15, 16, 17]. The main avenue for such expansions are gene duplications [18, 19, 20, 21], which generate copies of the TFs and thus provide the "raw material" for evolutionary diversification. Subsequent specialization of TFs often involves divergence in both their inputs (e.g., ligands) and outputs (regulated genes) [22, 3]. Examples range from metabolic repressors involved in bacterial carbon metabolism that arose from the same ancestor via a series of duplication-divergence events [23], and ancestral TF Lys14 in the metabolism of *S. cerevisiae*, which diverged into 3 different TFs regulating different subsets of genes in *C. albicans* [24], to many variants of Lim and Pou-homeobox genes involved in neural development across different organisms [25]. In some systems the ligand sensing and gene regulatory functions are distributed across two or more molecules, as for bacterial two-component pathways [26] and eukaryotic signaling cascades [27]; here, too, specialization can occur by a series of mutations in multiple relevant components.

Immediately following a duplication event, molecular recognition between TFs, their input signals, and their binding sites is specific but undifferentiated between the two TF copies. Under selection to specialize, recognition sequences and ligand preferences of the two TFs can diverge, but only if some degree of matching between TFs and their binding sites is continually retained to ensure network function. Binding sites are thus forced to coevolve in tandem with the TFs, yet

little is known about the resulting limits to evolutionary outcomes and their dependence on important parameters: the number of regulated genes, the length and specificity of the binding sites, the correlations between the input signals, and so on.

Theoretical understanding of TF duplication is still incomplete, with existing models predominantly belonging to two categories. The first category of gene duplication-differentiation models studies subfunctionalization of isolated proteins (e.g., enzymes) that do not have any regulatory role [28]. When cis-regulatory mutations that control the expression of the duplicated gene are included [29, 30, 31, 32, 33], this is done in a simplified fashion, e.g., by a small number of discrete alleles that represent TF binding sites appearing and disappearing at fixed rates [32, 33]. Because this approach ignores the essentials of molecular recognition, it cannot model co-evolution between TFs and their binding sites—the topic of our interest.

The second category of studies tracks regulatory sequences explicitly and uses a biophysical description of TF-BS (binding site) interactions, properly accounting for the fact that TFs can bind a variety of DNA sequences with different affinities [34, 35, 36]. In conjunction with thermodynamic models of gene regulation [37, 38, 39, 40], this approach has been used to study the evolution of binding sites given a single TF [41, 42, 36, 43, 44], while mostly overlooking the issue of TF duplication and subfunctionalization (but see [45, 46]).

Here we synthesize these two frameworks—the biophysical description of gene regulation and the evolutionary modeling of TF specialization—to construct a realistic description of the fundamental step by which regulatory networks have evolved. A biophysical model of this setup gives rise to complex fitness landscapes that are markedly different from simple forms considered previously; in what follows, we show that realistic landscapes exert a major influence over the evolutionary outcomes and dynamics.

Results

A biophysically realistic fitness landscape

In our model, N_{TF} transcription factors regulate N_G genes by binding to sites of length L base pairs; for simplicity, we consider each gene to have one such binding site. The specificity of a TF for any sequence is determined by the TF's preferred (consensus) sequence; sequences matching consensus are assigned lowest energy, $E = 0$, which corresponds to tightest binding, and every mismatch between the consensus and the binding site increases the energy by ϵ; this additive "mismatch"

model has a long history in gene regulation literature [47, 48, 42, 34].

The equilibrium probability that the binding site of gene j ($j = 1, \ldots, N_G$) is bound by active TFs of type i ($i = 1, \ldots, N_{\rm TF}$) is a proxy for the gene expression level and is given by the thermodynamic model of gene regulation [37, 49]:

$$p_{jm}(\{k_{ij}\}, \{C_i(m)\}) = \frac{\sum_i C_i(m) e^{-\epsilon k_{ij}}}{1 + \sum_i C_i(m) e^{-\epsilon k_{ij}}}, \tag{1}$$

where $C_i(m)$ is dimensionless concentration of active TFs of type i in condition m, k_{ij} is the number of mismatches between the consensus sequence of the i-th TF species and the binding site of the j-th gene, and ϵ is the energy per mismatch in units of $k_B T$. Concentration $C_i(m)$ of active TFs depends on condition m, which can represent either time or space (e.g., during developmental gene expression programs) or a discrete external environment (e.g., the presence/absence of particular chemical signals). The simplest case considered here assumes the existence of two such signals that can be either present or absent, in any combination, for a total number of 4 possible environments ($m = 00, 01, 10, 11$), occurring with probabilities α_m; an important parameter will be the correlation, $-1 \leq \rho \leq 1$, between the two signals. Each TF has two binary alleles, $\sigma_i \in [00, 01, 10, 11]$, specifying its sensitivity to the two signals. If the TF i is responsive to a signal and that signal is present in environment m, then its active concentration $C_i(m) = C_0$; otherwise, $C_i(m) = 0$. Given constants C_0, ϵ, and the genotype $\mathcal{G}$—comprising TF consensus and binding site sequences as well as TF sensitivity alleles σ_i—the thermodynamic model of Eq. (1) fully specifies expression levels for all genes in all environments.

Fig 1A illustrates this setup for a simple case $N_{\rm TF} = N_G = 2$, assuming that the two copies of the TF emerged through an initial gene duplication event and are fixed in the population. The original TF regulates two downstream genes by binding to their binding sites. It is sensitive to both external signals, which can be present with a varying degree of correlation (Fig 1B). After duplication, three types of mutation can occur, as shown in Fig 1C: point mutations in the binding sites (rate μ), mutations in the TF coding sequence that change TF's preferred (consensus) specificity (rate $r_{\rm TF}\mu$), and mutations in the two signal-sensing alleles (rate $r_{\rm S}\mu$), which can give each TF specificity to both signals, to one of them, or to neither. An example in Fig 1D shows the state of the system after several mutations have affected the degree of (mis)match between the TFs and the binding sites, k_{ij}; an especially important quantity that tracks the overall divergence of the TF specificity is denoted as M, the match between the two TF consensus sequences.

To complete the evolutionary model, a fitness function is required. We assume selection for

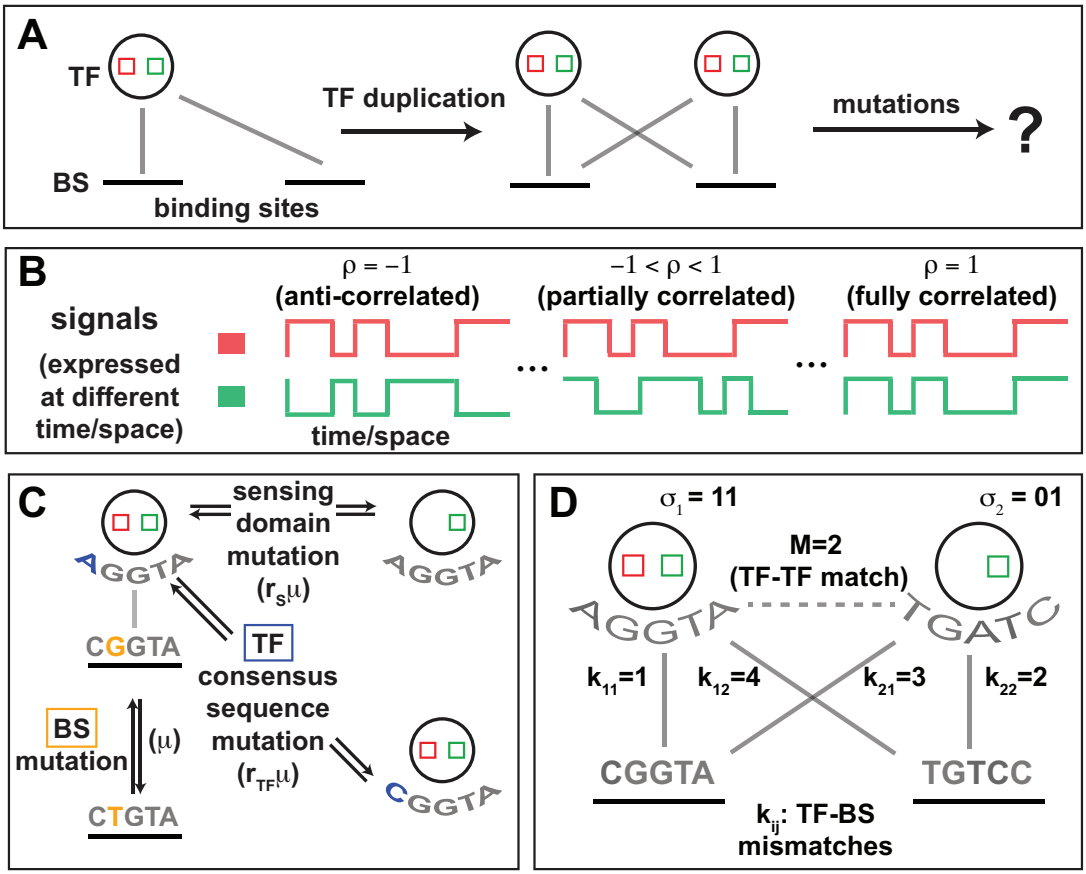

Figure 1: **Schematic of the model. (A)** TF, initially responsive to two external signals (red and green "slots") and regulating two genes, duplicates and the additional copy fixes in the population. Immediately after duplication, the two copies are undifferentiated. **(B)** A crucial parameter that will determine the fate of the duplicate is the correlation, ρ, of the two signals that activate or induce expression of the TFs. The signals can correspond to different time periods in development, spatial regions in the organism or tissue, or external conditions / ligands. **(C)** Various mutation types that can occur post-duplication with their associated rates. **(D)** After accumulating several mutations, the pattern of mismatches between TF consensus sequences and the binding sites is reflected in new values of $\{k_{ij}\}$, which determine the activation levels of the two genes according to Eq. (1). M, the number of matches between the consensus sequences of the two TFs (with a value between 0 and L), keeps track of the overall divergence of the TF specificities.

the genes to acquire distinct expression patterns in response to external signals, and thus define this fully specialized state as having the highest fitness in our model. Specifically, we penalize the deviations in actual gene expression, p_{jm}, from the ideal expression levels, p^*_{jm}:

$$F = -s \sum_j \sum_m \alpha_m \beta_{jm} (p_{jm} - p^*_{jm})^2, \tag{2}$$

where the ideal expression level p^*_{jm} is 1 (fully induced) for the first gene if signal 1 is present and the expression is 0 (not induced) otherwise, and similarly for the second gene; β_{jm} can be used to vary the relative weight of different errors (e.g. of a gene being uninduced when it should be induced and vice versa), and s is the selection intensity. Importantly, selection does not directly depend on the TFs, but only on the expression state of the genes they regulate; genes, however, can only be expressed when TFs bind to proper binding sites, implicitly selecting on TFs.

We take mutation rates to be low enough that a beneficial mutation fixes before another beneficial mutation arises [50], allowing us to assume that the population is almost always fixed. The probability that the population occupies a particular genotypic state, $P(\mathcal{G}, t)$, evolves according to a continuous-time discrete-space Markov chain that specifies the rate of transition between any two genotypes; the transition rates are a product between the mutation rates between different states and the fixation probability that depends on the fitness advantage a mutant has over the ancestral genotypes [51, 42]. The size of genotype space is high-dimensional but still tractable, because our model only requires us to keep track of mismatches and not full sequences, i.e., to write out the dynamical equations for quantities $\{M, k_{ij}, \sigma_i\}$; standard Markov chain techniques can then be used to compute the evolutionary steady state, first hitting times to reach specific evolutionary outcomes, or to perform stochastic simulations.

Fig 2 shows the interplay of biophysical constraints that give rise to a realistic fitness landscape for our problem. Given a match, M, between two TF consensus sequences, only certain combinations of mismatches, (k_{1j}, k_{2j}), of the TFs with each of the two binding sites are possible. A particular allowed combination can be realized by different number of genotypes, as shown in Fig 2A, providing a detailed account of the entropy of the neutral distribution. For each of the four environments, Eq. (1) predicts gene expression at every pair of mismatch values (Fig 2B); together with the probabilities of different environments occurring, the gene expression pattern determines the genotypes's fitness, F. TF specialization then unfolds on this landscape by different types of mutations (e.g., Fig 2C). Although the landscape is complex and high-dimensional, it is highly structured and ultimately fully specified by only a handful of biophysical parameters. Furthermore, because of

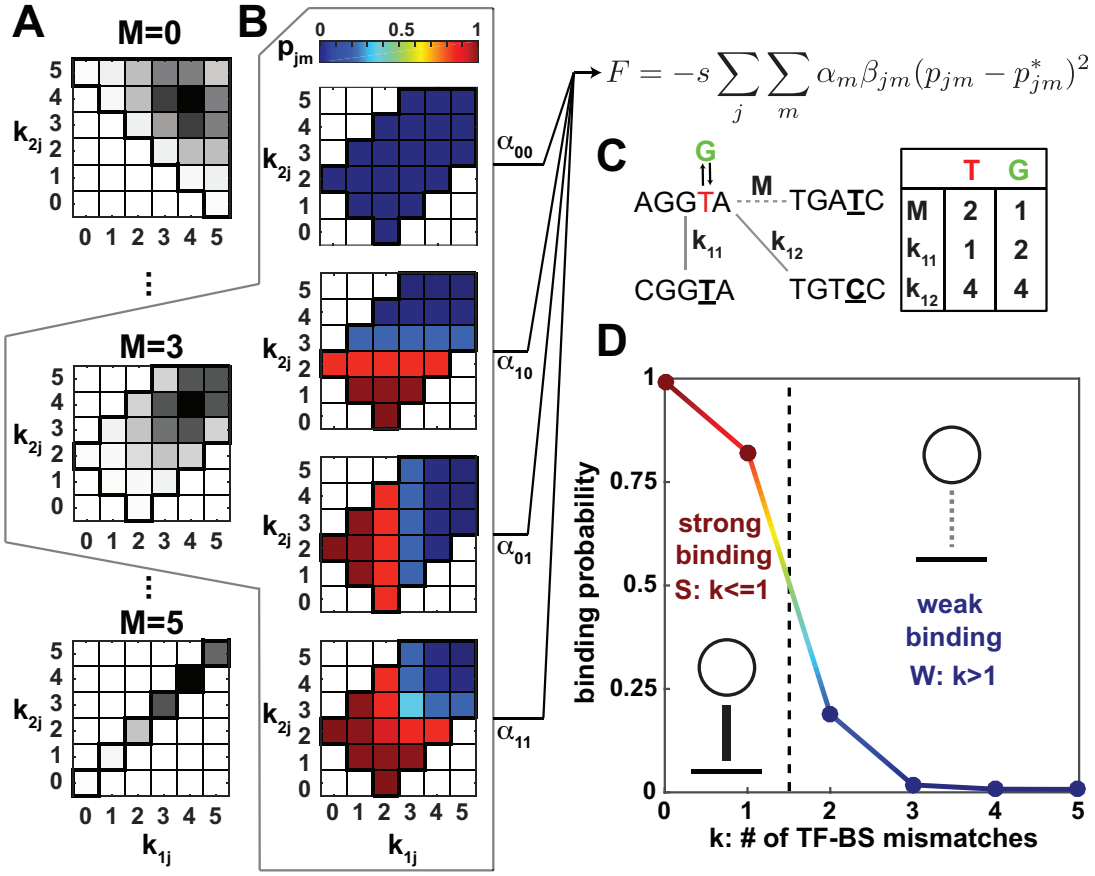

Figure 2: **Biophysical and evolutionary constraints shape the genotype-phenotype-fitness map after TF duplication. (A)** Match, M, between transcription factor consensus sequences (here, of length $L = 5$), constrains the possible mismatch values, k_{1j}, k_{2j}, between the gene's binding site and either TF. For example, when the two TFs are identical ($M = L = 5$, bottom left), they must have equal mismatches with all genes ($k_{1j} = k_{2j}$). Some combinations of mismatches are impossible given M (white), while others are realized by different numbers of genotypes (grayscale). **(B)** Expression level (color) for a regulated gene given all mismatch combinations, k_{1j}, k_{2j}, at $M = 3$. Impossible mismatch combinations are white. Each of the four panels shows expression levels in four possible environments, $m = 00, 10, 01, 11$. Fitness F depends on the structure of mismatches (A), the biophysics of binding (B), and the frequencies of different environments, α_m. Here we choose α so that the marginal probability of each input signal is always $\frac{1}{2}$ but the correlation can be varied, and assign weight $\beta_{jm} = 1$ whenever the gene should be induced but is not, and $\beta_{jm} = \frac{1}{2}$ when it should not be induced but is. **(C)** A single point mutation, e.g. a change in one TF's binding specificity from T to G, can simultaneously affect the match, M, and either increase, decrease, or leave intact the mismatches, k_{11} and k_{12}, that determine fitness. **(D)** TF-BS interactions with mismatch k that is low enough to ensure a high binding probability ($p > 1/2$) are assigned to a "strong binding" phenotype (black link); conversely, $p < 1/2$ is a "weak binding" phenotype (dotted link).

the sigmoidal shape of binding probability as a function of mismatch k [Eq. (1)], it is possible to assign phenotypes of "strong" and "weak" binding to every TF-BS interaction, allowing us to depict network interactions graphically, as shown in Fig 2D, and to classify the possible macroscopic evolutionary outcomes, as we will show next.

Evolutionary outcomes in steady state

Evolutionary outcomes in steady state are determined by a balance between selection and drift. The steady state distribution over genotypes is [52]

$$P_{\mathrm{SS}}(\mathcal{G}) = P(\mathcal{G}, t \to \infty) = P_0(\mathcal{G}) \exp(2NF(\mathcal{G})), \tag{3}$$

where P_0 is the neutral distribution of genotypes and N is the population size. Eq. (3) is similar to the energy/entropy balance of statistical physics [53], with fitness F playing the role of energy and $\log P_0$ the role of entropy; in our model, both of these quantities are explicitly computable, as is the resulting steady state distribution.

Understanding the high dimensional distribution over genotypes is difficult, but classification of individual TF-BS interactions into "strong" and "weak" ones, as described above, allows us to systematically and uniquely assign every genotype to one of a few possible macroscopic outcomes, or "macrostates," graphically depicted in Fig 3A. Thus, in the `No Regulation` state, input signals are not transduced to the target genes, either because TF-BS mismatches are high and there is no binding or because TFs themselves lose responsiveness to the input signals; in the `One TF Lost` state, a single TF regulates both genes (as before duplication), while the other TF is lost, i.e., its specificity has diverged so far that it does not bind any of the sites; the `Specialize Binding` state corresponds to each TF regulating its own gene without cross-regulating the other but the signal sensing domains are not yet signal specific, as they are in the `Specialize Both`, the state which we have defined to have the highest fitness. Finally, the `Partial` macrostate predominantly features configurations where each of the TFs binds at least one binding site, but one of the TFs still binds both sites or retains responsiveness for both input signals; functionally, these configurations lead to large "crosstalk," where input signals are non-selectively transmitted to both target genes.

Ultimately, these macrostates are the functional network phenotypes that we care about. The number of genotypes in each macrostate, however, can vary by orders of magnitude; for example, the `No Regulation` state is larger by $\sim 10^4$ relative to the high-fitness `Specialize Both` state, for our baseline choice of parameters ($L = 5, \epsilon = 3$). Selection can act against this strong entropic

bias, and the distribution of fitness values across genotypes within each macrostate is shown in Fig 3B. Clearly, the mean or median fitness within each macrostate is a poor substitute for the detailed structure of fitness levels that depend nonlinearly on TF-BS mismatches and the degeneracy of the sequence space. Unlike the entropic term in Fig 3A, fitness also depends on the statistics of the environment, α_m, and in particular, the correlation ρ between the two signals. For example, when the signals are strongly correlated, the `Initial` state right after duplication or the `One TF Lost` state can achieve quite high fitnesses, since responding to the wrong signal or having a high degree of crosstalk will still ensure largely appropriate gene expression pattern in all likely environments. In contrast, at strong negative correlation, many genotypes in `Specialize Binding` and `Initial` states will suffer a large fitness penalty because their sensing domains are not specialized for the correct signals, while the `Specialize Both` state will have high fitness regardless of the environmental signal correlation.

How do fitness and entropy combine to determine macroscopic evolutionary outcomes? Fig 3C shows the most probable macrostate as a function of selection strength and signal correlation. At weak selection, specific TF-BS interactions cannot be maintained against mutational entropy and the system settles into the most numerous, `No Regulation` state. Higher selection strengths can maintain a limited number of TF-BS interactions in `Partial` states. Beyond a threshold value for Ns, the evolutionary outcome depends on the signal correlation: when signals are anti-correlated or weakly correlated, the TFs reach the fully specialized state, whereas high positive correlation favors losing one TF and having the remaining TF regulate both genes and respond to both signals. As signal correlation increases, so does the selection strength required to support full specialization.

The map of evolutionary outcomes is very robust to parameter variations. The energy scale of TF-DNA interactions is that of hydrogen bonds: $\epsilon \sim 3$ (in k_BT units), consistent with direct measurements. The scale of C_0 is set to ensure that consensus sites are occupied at saturation while fully mismatching sites are essentially empty. The only remaining important biophysical parameter is L, the length of the binding sites. As expected, increasing L expands the regions of `No Regulation` and `Partial` at low Ns, due to entropic effects. Surprisingly, however, one can demonstrate that the important boundary between the `Specialize` and `One TF Lost` states is independent of L; furthermore, the map in Fig 3C is exactly robust to the overall rescaling of the mutation rate, μ, and even to separate rescaling of individual rates $r_{\rm S}, r_{\rm TF}$.

We compare the steady-state marginal distributions of TF-BS mismatches and the match, M, between the two TFs, under strong selection to specialize ($Ns = 25$) vs neutral evolution ($Ns = 0$). Mismatch distributions for k_{11} and k_{21} in Fig 3D display a clear difference in the two regimes:

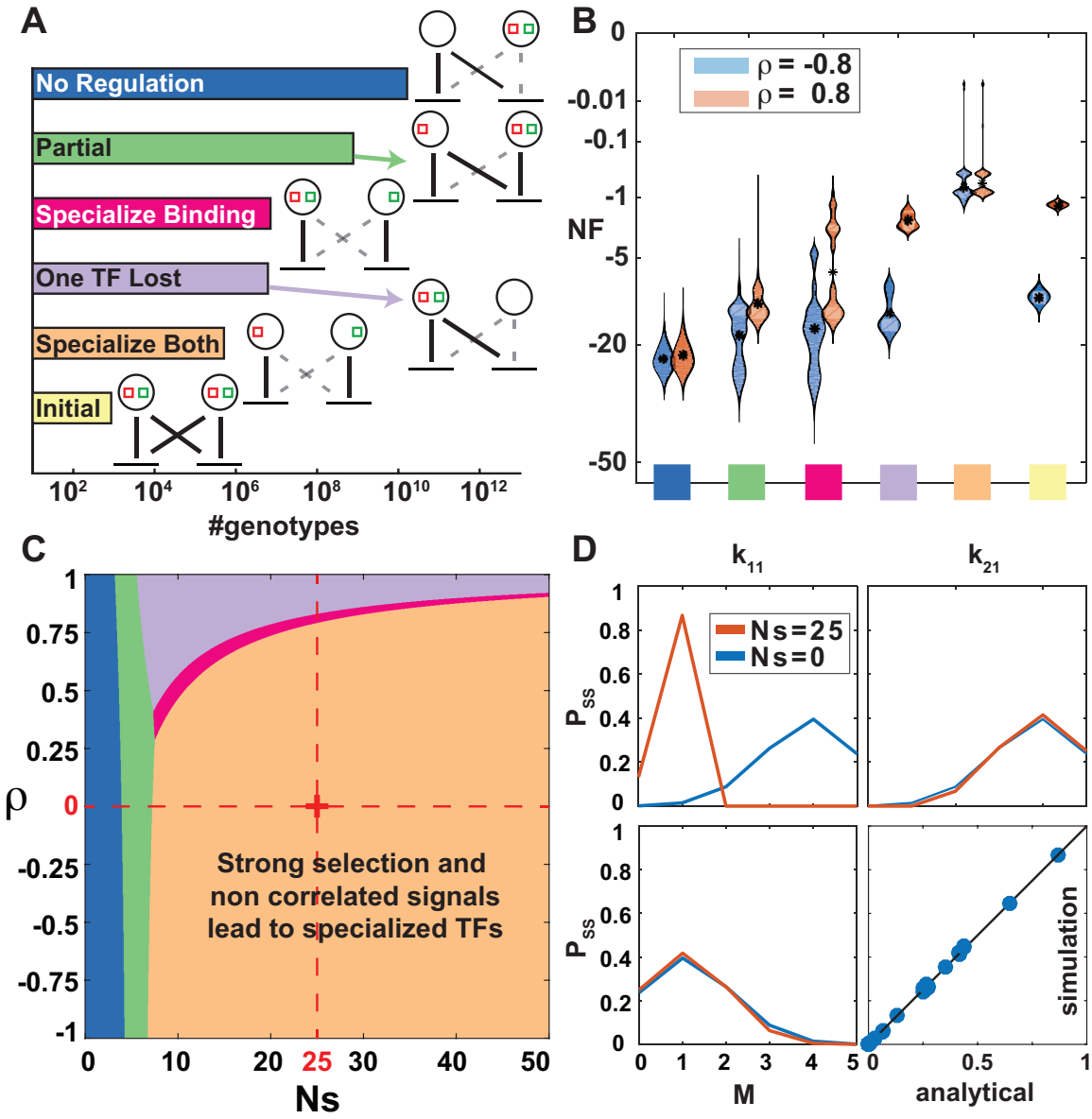

Figure 3: **Steady state evolutionary outcomes of TF duplication. (A)** Evolutionary macrostates (see text) depicted graphically as network phenotypes with lines indicating TF-BS interactions. Logarithmic scale indicates the number of genotypes in each macrostate. **(B)** Distribution of fitness values across genotypes in each macrostate (color-coded as in A), shown as violin plots, for two values of signal correlation, ρ. Black dots = median fitness in the macrostate. **(C)** Most probable outcome of gene duplication in steady state (color-coded as in A), as a function of selection strength, Ns, and the correlation between two external signals, ρ. **(D)** Steady state distributions for mismatches ($P_{\rm SS}(k_{ij}|\sigma_1 = 10, \sigma_2 = 01)$, upper row) and the match between the two TF consensus sequences ($P_{\rm SS}(M|\sigma_1 = 10, \sigma_2 = 01)$, lower left), under strong selection (red; at baseline parameters denoted by the red cross in C) and neutrality (blue; Bernoulli distributions). Comparison between analytical calculation and 400 replicates of the stochastic simulation (lower right). Here and in subsequent figures, baseline parameters are $L = 5$, $\epsilon = 3$, $r_{\rm S} = r_{\rm TF} = 1$.

strong selection favors a small mismatch of the BS with the cognate TF, sufficient to ensure strong binding but nonzero due to entropy, and a large mismatch with the noncognate TF, to reduce crosstalk. Surprisingly, however, the distribution of matches M between two TF consensus sequences shows only a tiny signature of selection, with both distributions peaking around 1 match. As a consequence, inferring selection to specialize from measured binding preferences of real TFs might not be feasible with realistic amounts of data.

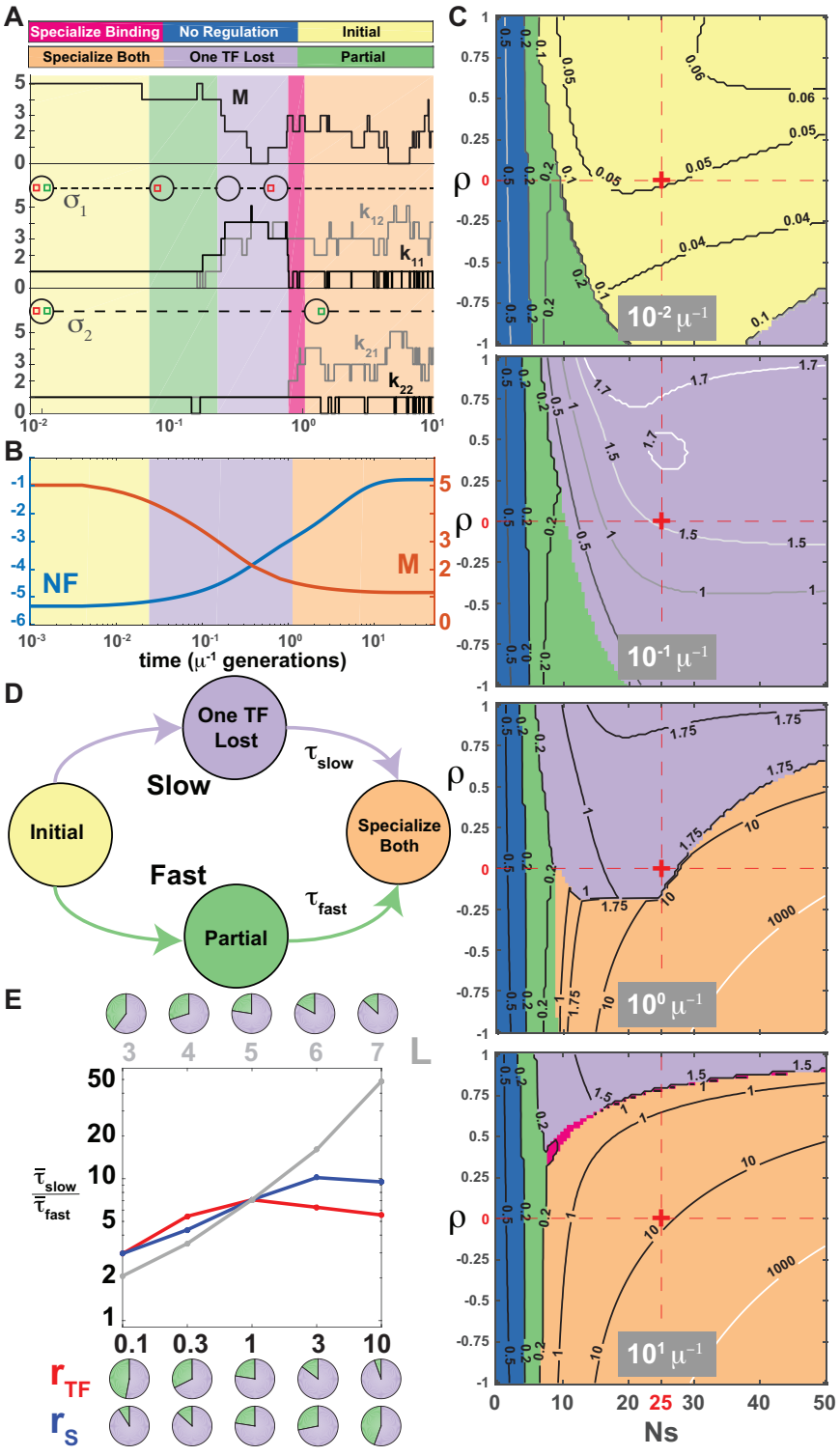
A
Specialize Binding
No Regulation
Initial
Specialize Both
One TF Lost
Partial
M
σ1
k12
k11
σ2
k21
k22
B
NF
M
time (μ-1 generations)
C
ρ
10-2 μ-1
10-1 μ-1
100 μ-1
101 μ-1
Ns
D
One TF Lost
Slow
τslow
Initial
Specialize Both
Fast
τfast
Partial
E
L
τslow / τfast
rTF
rS

Figure 4: **Slow and fast pathways to TF specialization. (A)** Temporal traces of TF-TF match M (top), and TF-BS mismatches k_{ij} (middle: TF1, bottom: TF2) with the corresponding signal specificity mutations denoted on dashed lines, for one example evolutionary trajectory at baseline parameters. Macrostates are color-coded as in the top legend and Fig 3. **(B)** Average dynamics of fitness NF (blue, left scale) and TF-TF match M (red, right scale). For every timepoint, the dominant macrostate is denoted in color. **(C)** Snapshots of dominant macrostates (at increasing time post-duplication as indicated in the panels), shown for different combinations of selection strength Ns and signal correlation ρ as in Fig 3. Contours mark dwell times in the dominant macrostates (in units of μ^{-1}). Red cross = baseline parameters. **(D)** Schematic of the two alternative pathways to specialization. $\tau_{\rm slow}$ and $\tau_{\rm fast}$ are the total times to specialization for the "slow" and the "fast" pathway, respectively. **(E)** Relative duration of the two pathways, as a function of binding site length L (gray line, top axis), TF consensus sequence mutation rate $r_{\rm TF}$ (red), and signal domain mutation rate $r_{\rm S}$ (blue, bottom axis). Pie charts indicate the fraction of slow (pink) and fast (green) pathways at each parameter value.

Evolutionary dynamics and fast pathways towards specialization

Next, we focus on evolutionary trajectories and the timescales to reach the fully specialized state after gene duplication. An example trajectory is shown in Fig 4A: the two TFs start off identical (with maximal match, $M = L = 5$) until, as a result of the loss of specificity for both signals, TF1 starts to drift, diverging from TF2 (sharply decreasing M in `One TF Lost` state) and losing interactions with both binding sites. Subsequently TF1 reacquires preference to the red signal, which drives the reestablishment of TF1 specificity for one binding site during a short `Specialize Binding` epoch, followed quickly by the specialization of TF2 for the green signal at the start of `Specialize Both` epoch of maximal fitness.

Dynamics of the TF-TF match, M, and the scaled fitness, NF, become smooth and gradual when discrete transitions and the consequent large jumps in fitness are averaged over individual realizations, as in Fig 4B. Importantly, we learn that the sequence of dominant macrostates leading towards the final (and steady) state, `Specialize Both`, involves a long intermediate epoch when the system is in the `One TF Lost` state. We examine this sequence of most likely macrostates in detail in Fig 4C, and visualize it analogously to the map of evolutionary outcomes in steady state shown in Fig 3C. High Ns and correlation (ρ) values favor trajectories passing through the `One TF Lost` state, while intermediate Ns ($5 \lesssim Ns \lesssim 20$) and low correlation values enable transitions through `Partial` macrostate; along the latter trajectory, the binding of neither TF is completely abolished. Typical dwell times in dominant states, indicated as contours in Fig 4C, suggest that specialization via the `One TF Lost` state should be slower than through the `Partial` state, which is best seen at $t = 1/\mu$, where specialization has already occurred at intermediate Ns and low, but

not high, ρ values.

It is easy to understand why pathways towards specialization via the `One TF Lost` state are slow. As the example in Fig 4A illustrates, so long as one TF maintains binding to both sites and thus network function (especially when signals are strongly correlated), the other TF's specificity will be unconstrained to neutrally drift and lose binding to both sites, an outcome which is entropically highly favored. After the TF's sensory domain specializes, however, the binding has to re-evolve essentially from scratch in a process that is known to be slow [44] unless selection strength is very high. In contrast to this "Slow" pathway, the "Fast" pathway via the `Partial` state relies on sequential loss of "crosstalk" TF-BS interactions, with the divergence of TF consensus sequences followed in lock-step by mutations in cognate binding sites. Specifically, the likely intermediary of the fast pathway is a `Partial` configuration in which the first TF responds to both signals but only regulates one gene, whereas the second TF is already specialized for one signal, but still regulates both genes.

The fast and the slow pathways are summarized in Fig 4D. A detailed analysis reveals how different biophysical and evolutionary parameters change the relative probability and the average duration (Fig 4E) of both pathways. For example, increasing the length, L, of the binding sites favors the slow pathway as well as drastically increases its duration, leading to very slow evolutionary dynamics. Increasing the rate of TF-specificity-affecting mutations, r_{TF}, has a qualitatively similar effect, while increasing the mutation rate affecting the sensory domain, r_{S}, favors the fast pathway. Indeed, in the limit when r_{S} is much larger than the other two mutation rates, the sensing domain specializes almost instantaneously, making the complete loss of binding by either TF very deleterious and thus avoiding the `One TF Lost` state; the adaptation dynamics is initially rapid, with binding sites responding to diverging TF consensus sequences, and subsequently slow, when TF consensus sequences further minimize their match, M, in a nearly neutral process.

Promiscuity-promoting mutations

Typically, each TF must regulate more than one target gene. As the number of regulated genes per TF ($n_G = N_G/N_{\mathrm{TF}}$) increases, intuition suggests that the evolution of the TF's consensus sequence should become more and more constrained: while a mutation in an individual binding site can lower the total fitness by increasing mismatch and thereby impeding TF-BS binding, a single mutation in the TF's consensus has the ability to simultaneously weaken the interaction with many binding sites, leading to a high fitness penalty. Our analysis of the biophysical fitness land-

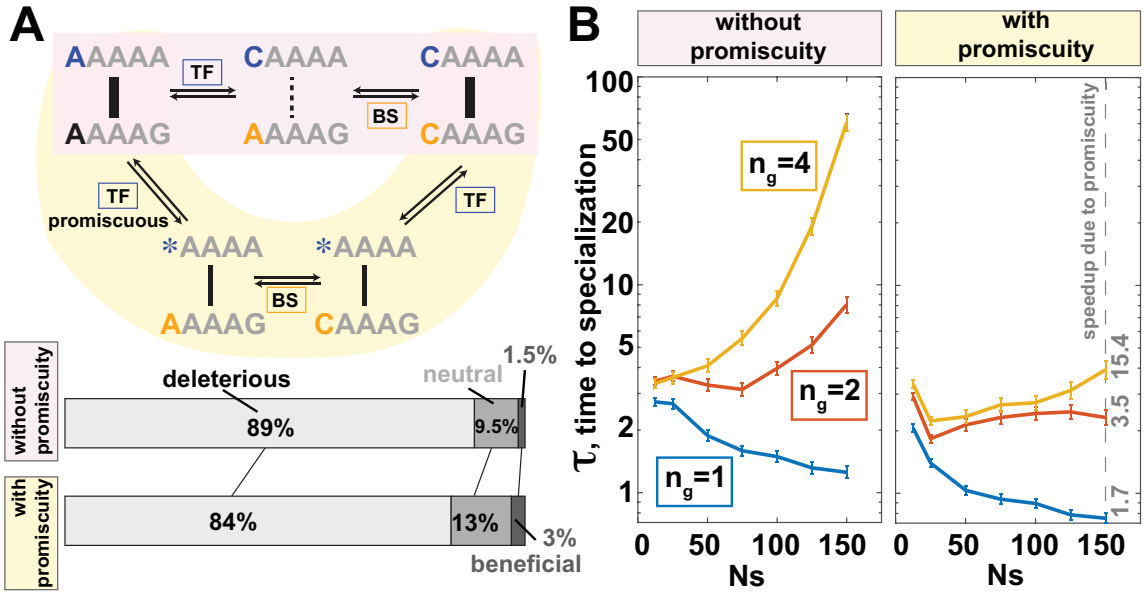

Figure 5: **Promiscuity-promoting mutations speed up specialization with multiple regulated genes per TF. (A)** In the absence of promiscuity-promoting mutations, a compensatory series of point mutations in the TF's consensus (upper sequence) and its binding site (lower sequence) is needed to maintain TF-BS specificity (top; light red). Alternatively, in the presence of promiscuity-promoting mutations in the TF consensus, a position in the TF's recognition sequence (marked by a star) can lose and later regain sequence specificity (middle; light yellow). Promiscuity decreases the fraction of deleterious mutations along typical pathways to specialization (bottom, computed using baseline parameters). **(B)** Time to specialization as a function of selection strength, Ns, without (left) and with (right) promiscuity promoting mutations in the TF, for different numbers of regulated genes per TF, n_g (color).

scape confirmed that the landscape gets progressively more frustrated as the number of regulated genes per TF increases, due to the explosion of constraints that TFs have to satisfy to ensure the maintenance of functional regulation. Consequently, one can expect extremely long times to specialization. How can it nevertheless proceed at observable rates?

Energy matrices for many real TFs display "promiscuous" specificity where, at a particular position within the binding site, binding to multiple nucleotides is equally preferable. We wondered how our findings would be affected if consensus sequence specificity of the TFs could pass through such intermediate promiscuous states. Fig 5A shows how TF consensus sequence and the corresponding binding site can co-evolve using point mutations, or using the new "promiscuity-promoting" mutation type for the TF: promiscuity-promoting mutation renders one position in the recognition sequence of the TF insensitive to the corresponding DNA base in the binding site. Evolutionary pressure on the binding sites is therefore temporarily relieved, until the specificity of the TF is reestablished by a back mutation. Without promiscuity-promoting mutations, TF-

BS co-evolution must proceed in a tight sequence of compensatory mutations; with promiscuity-promoting mutations, such a precise sequence is no longer required, although one extra mutation is needed to reestablish high TF-BS specificity. With promiscuity, the fraction of deleterious mutations along the evolutionary path towards specialization is reduced. As shown in Fig 5B, this has drastic effects on the time to specialization. Without promiscuity, increasing the selection strength, Ns, decreases the required time when each TF regulates one gene, as expected for a landscape with large neutral plateaus but with no fitness barriers. For $n_g > 1$, however, the landscape develops barriers that need to be crossed, and evolutionary time starts increasing with Ns. In contrast, promiscuity enables fast emergence of TF specialization even with multiple regulated genes in a broad range of evolutionary parameters (although there are also costs due to high promiscuity).

Discussion

The role that the shape of a fitness landscape plays for the dynamics and the final outcomes of evolution has been appreciated in population genetics for a long time. This has stimulated a large body of theoretical research into evolution on toy model landscapes [54, 55], as well as motivated efforts to map out real, small-scale landscapes experimentally. For limited classes of problems, mostly those involving molecular recognition, biophysical constraints are informative enough to permit computational exploration of complex landscapes. Such is the case for the secondary structure of RNA [56], antibody-antigen interactions, protein-protein interactions, and transcription factor-DNA binding, explored here. We exploit this prior knowledge to construct a fitness landscape for a more complicated evolutionary event, the specialization of two TFs after duplication, a key evolutionary step by which gene regulatory networks expand. The biophysical model naturally captures a number of essential features, without having to introduce them "by hand": the fact that specialization is driven by avoidance of regulatory crosstalk; the importance of the mutational entropy; the dependence on number of downstream genes; the existence of transient network configurations preceding specialization, which crucially impact dynamics; and the importance for evolutionary outcomes of the statistical properties of the signals that TFs respond to. Importantly, the expressive power of our framework does not come at increased modeling cost: while complex, the fitness landscape is still determined only by a few, mostly known, parameters, and an exponentially large space of genotypes can be systematically coarse grained to a small set of functional network phenotypes. This combination of biophysical and co-evolutionary approaches is applicable generally to the evolution of molecular interactions, e.g., in protein interaction networks.

In steady state, our results robustly identify correlation between the environmental signals that drive TFs as a key determinant for specialization, as shown in Fig 3C. Unless the new signal, for which a post-duplication TF can specialize, is sufficiently independent (uncorrelated) from the existing signals that the regulatory network processes, one TF copy will be lost due to drift. As a consequence, the *effective dimensionality of environmental signals* dictates the complexity of genetic regulatory networks [57], reminiscent of information-theoretic tradeoffs in sensory neuroscience; in evolutionary terms, selection to maintain complex regulation needs to withstand the mutational flux into vastly more numerous but less functional network phenotypes. Recently, it has been shown that finite biochemical specificity also limits the complexity of genetic regulatory networks [58]; an interesting direction for future research is to understand how the balance between regulatory crosstalk, environmental signal statistics, and evolutionary constraints ultimately determines the number of TFs that can be stably maintained. A related question concerns the expected match between pairs of TFs in a large network as a signature of selection for specialized function; for an isolated pair of TFs, our results in Fig 3D predict only a tiny deviation from neutrality.

Timescales and pathways to specialization are completely shaped by the properties of the biophysical fitness landscape, and thus cannot be captured by simple allelic models that ignore the topology of the sequence space. We show that the fast pathway to specialization transitions through `Partial` states where neither of the two TFs completely loses binding. Interestingly, it is exactly the existence of crosstalk interactions that permits fast adaptation via these transient states, by maintaining the network function through one TF, while the other is free to diverge in a series of mutations to the TF and its future binding site [59]. Crosstalk thus enables some amount of network plasticity during early adaptation, yet is ultimately selected against, when TFs become fully specialized [60, 61]. In the protein-protein-interaction literature, `Partial` states are sometimes referred to as promiscuous states, and they have been suggested as evolutionarily accessible intermediaries that relieve the two interacting molecules of the need to evolve in a tight (and likely very slow) series of compensatory mutations [62]. In contrast to the fast pathway, the slow pathway involves a complete loss of TF-BS binding interactions; the long timescale emerges from long dwell times while the TF and the binding sites evolve in a nearly neutral landscape before TF-BS specificity is reacquired. Long binding sites and (perhaps counter-intuitively) fast TF mutation rates favor the slow pathway, while fast sensing domain mutation rates favor the fast pathway.

The situation changes qualitatively when each TF regulates more genes [63]. On the one hand, entropy makes pathways that pass through the `One TF Lost` state dynamically uncompetitive, as multiple binding sites would have to emerge *d*e novo to reestablish interactions with a diverged TF.

This would favor fast pathways through `Partial` states. On the other hand, the biophysical fitness landscape develops frustration (or sign epistasis) as $n_g > 1$ and the timescales to specialization lengthen with increasing selection strength when passing through `Partial` and `One TF Lost` states. We demonstrate that frustration is relieved by promiscuity-promoting mutations in the transcription factor, enabling fast emergence of specialization even with multiple regulated genes.

Taken together, our results paint a picture of TF specialization that most likely proceeds through intermediate states with high crosstalk, in which one TF has already specialized for its input signals but not yet for the target genes, while the other TF is not yet specialized for the input signals but only regulates one gene. In addition, these intermediate states are likely to be more promiscuous, binding different sites with the same affinity, with the promiscuity reverting to specific binding towards the end of specialization. This picture is qualitatively different from the paradigmatic idea of a simple and sequential progression of compensatory mutations in the TF and its binding sites [64, 45]. It depends fundamentally on the biophysical model of TF-BS interactions, predicts significantly faster specialization times, as well as the existence of promiscuous TF variants that are starting to be observed in genomic analyses of duplication-specialization events [14, 15].

Acknowledgments We thank the People Programme (Marie Curie Actions) of the European Union's Seventh Framework Programme (FP7/2007-2013) under REA grant agreement Nr. 291734 (T.F.), ERC grant Nr. 250152 (N.B.), and Austrian Science Fund grant FWF P28844 (G.T.).

References

[1] King MC, Wilson AC (1975) Evolution at two levels in humans and chimpanzees. *Science* 188(4184):107–116.

[2] Gilad Y, Oshlack A, Smyth GK, Speed TP, White KP (2006) Expression profiling in primates reveals a rapid evolution of human transcription factors. *Nature* 440(7081):242–245.

[3] Wray GA (2007) The evolutionary significance of cis-regulatory mutations. *Nature Reviews Genetics* 8(3):206–216.

[4] Carroll SB (2005) Evolution at Two Levels: On Genes and Form. *PLoS Biol* 3(7):e245.

[5] Yona A, Frumkin I, Pilpel Y (2015) A Relay Race on the Evolutionary Adaptation Spectrum. *Cell* 163(3):549–559.

[6] Madan Babu M, Teichmann SA, Aravind L (2006) Evolutionary Dynamics of Prokaryotic Transcriptional Regulatory Networks. *Journal of Molecular Biology* 358(2):614–633.

[7] Kacser H, Beeby R (1984) Evolution of catalytic proteins: On the origin of enzyme species by means of natural selection. *Journal of Molecular Evolution* 20(1):38–51.

[8] Simionato E et al. (2007) Origin and diversification of the basic helix-loop-helix gene family in metazoans: insights from comparative genomics. *BMC Evolutionary Biology* 7:33.

[9] Larroux C et al. (2008) Genesis and Expansion of Metazoan Transcription Factor Gene Classes. *Molecular Biology and Evolution* 25(5):980–996.

[10] Hobert O, Carrera I, Stefanakis N (2010) The molecular and gene regulatory signature of a neuron. *Trends in neurosciences* 33(10):435–445.

[11] Achim K, Arendt D (2014) Structural evolution of cell types by step-wise assembly of cellular modules. *Current Opinion in Genetics & Development* 27:102–108.

[12] McKeown A et al. (2014) Evolution of DNA Specificity in a Transcription Factor Family Produced a New Gene Regulatory Module. *Cell* 159(1):58–68.

[13] Baker CR, Tuch BB, Johnson AD (2011) Extensive DNA-binding specificity divergence of a conserved transcription regulator. *Proceedings of the National Academy of Sciences* 108(18):7493–7498.

[14] Sayou C et al. (2014) A Promiscuous Intermediate Underlies the Evolution of LEAFY DNA Binding Specificity. *Science* 343(6171):645–648.

[15] Pougach K et al. (2014) Duplication of a promiscuous transcription factor drives the emergence of a new regulatory network. *Nature Communications* 5:4868.

[16] Nadimpalli S, Persikov AV, Singh M (2015) Pervasive Variation of Transcription Factor Orthologs Contributes to Regulatory Network Evolution. *PLOS Genet* 11(3):e1005011.

[17] Arendt D (2008) The evolution of cell types in animals: emerging principles from molecular studies. *Nature Reviews Genetics* 9(11):868–882.

[18] Ohno S (2013) *Evolution by gene duplication*. (Springer Science & Business Media).

[19] Magadum S, Banerjee U, Murugan P, Gangapur D, Ravikesavan R (2013) Gene duplication as a major force in evolution. *Journal of Genetics* 92(1):155–161.

[20] Andersson DI, Hughes D (2009) Gene Amplification and Adaptive Evolution in Bacteria. *Annual Review of Genetics* 43(1):167–195.

[21] Yona AH et al. (2012) Chromosomal duplication is a transient evolutionary solution to stress. *Proceedings of the National Academy of Sciences* 109(51):21010–21015.

[22] Wittkopp PJ, Kalay G (2012) Cis-regulatory elements: molecular mechanisms and evolutionary processes underlying divergence. *Nature Reviews Genetics* 13(1):59–69.

[23] Nguyen CC, Saier MH (1995) Phylogenetic, structural and functional analyses of the LacI-GalR family of bacterial transcription factors. *FEBS Letters* 377(2):98–102.

[24] Pérez JC et al. (2014) How duplicated transcription regulators can diversify to govern the expression of nonoverlapping sets of genes. *Genes & Development* 28(12):1272–1277.

[25] Hobert O, Westphal H (2000) Functions of LIM-homeobox genes. *Trends in Genetics* 16(2):75–83.

[26] Parkinson JS (1993) Signal transduction schemes of bacteria. *Cell* 73(5):857–871.

[27] Bowler C, Chua NH (1994) Emerging themes of plant signal transduction. *The Plant Cell* 6(11):1529–1541.

[28] Innan H, Kondrashov F (2010) The evolution of gene duplications: classifying and distinguishing between models. *Nature Reviews Genetics* 11(2):97–108.

[29] Force A et al. (1999) Preservation of Duplicate Genes by Complementary, Degenerative Mutations. *Genetics* 151(4):1531–1545.

[30] Lynch M, Force A (2000) The Probability of Duplicate Gene Preservation by Subfunctionalization. *Genetics* 154(1):459–473.

[31] Lynch M, O'Hely M, Walsh B, Force A (2001) The Probability of Preservation of a Newly Arisen Gene Duplicate. *Genetics* 159(4):1789–1804.

[32] Force A et al. (2005) The Origin of Subfunctions and Modular Gene Regulation. *Genetics* 170(1):433–446.

[33] Proulx SR (2012) Multiple Routes to Subfunctionalization and Gene Duplicate Specialization. *Genetics* 190(2):737–751.

[34] Maerkl SJ, Quake SR (2007) A Systems Approach to Measuring the Binding Energy Landscapes of Transcription Factors. *Science* 315(5809):233–237.

[35] Wunderlich Z, Mirny LA (2009) Different gene regulation strategies revealed by analysis of binding motifs. *Trends in Genetics* 25(10):434–440.

[36] Payne JL, Wagner A (2014) The Robustness and Evolvability of Transcription Factor Binding Sites. *Science* 343(6173):875–877.

[37] Shea MA, Ackers GK (1985) The OR control system of bacteriophage lambda: A physical-chemical model for gene regulation. *Journal of Molecular Biology* 181(2):211–230.

[38] Kinney JB, Murugan A, Callan CG, Cox EC (2010) Using deep sequencing to characterize the biophysical mechanism of a transcriptional regulatory sequence. *Proceedings of the National Academy of Sciences* 107(20):9158–9163.

[39] Sherman MS, Cohen BA (2012) Thermodynamic State Ensemble Models of cis-Regulation. *PLoS Comput Biol* 8(3):e1002407.

[40] He X, Samee MAH, Blatti C, Sinha S (2010) Thermodynamics-Based Models of Transcriptional Regulation by Enhancers: The Roles of Synergistic Activation, Cooperative Binding and Short-Range Repression. *PLoS Comput Biol* 6(9):e1000935.

[41] Berg J, Willmann S, Lässig M (2004) Adaptive evolution of transcription factor binding sites. *BMC Evolutionary Biology* 4:42.

[42] Lässig M (2007) From biophysics to evolutionary genetics: statistical aspects of gene regulation. *BMC Bioinformatics* 8(6):1–21.

[43] Lynch M, Hagner K (2015) Evolutionary meandering of intermolecular interactions along the drift barrier. *Proceedings of the National Academy of Sciences* 112(1):E30–E38.

[44] Tuğrul M, Paixão T, Barton NH, Tkačik G (2015) Dynamics of Transcription Factor Binding Site Evolution. *PLoS Genet* 11(11):e1005639.

[45] Poelwijk FJ, Kiviet DJ, Tans SJ (2006) Evolutionary potential of a duplicated repressor-operator pair: simulating pathways using mutation data. *PLoS computational biology* 2(5):e58.

[46] Burda Z, Krzywicki A, Martin OC, Zagorski M (2010) Distribution of essential interactions in model gene regulatory networks under mutation-selection balance. *Physical Review E* 82(1):011908.

[47] Von Hippel PH, Berg OG (1986) On the specificity of DNA-protein interactions. *Proceedings of the National Academy of Sciences* 83(6):1608.

[48] Gerland U, Moroz JD, Hwa T (2002) Physical constraints and functional characteristics of transcription factorDNA interaction. *Proceedings of the National Academy of Sciences* 99(19):12015–12020.

[49] Bintu L et al. (2005) Transcriptional regulation by the numbers: models. *Current Opinion in Genetics & Development* 15(2):116–124.

[50] Desai MM, Fisher DS (2007) Beneficial MutationSelection Balance and the Effect of Linkage on Positive Selection. *Genetics* 176(3):1759–1798.

[51] Kimura M (1962) On the Probability of Fixation of Mutant Genes in a Population. *Genetics* 47(6):713–719.

[52] Gillespie JH (2004) *Population Genetics: A Concise Guide*. (The Johns Hopkins University Press), 2nd edition.

[53] Sella G, Hirsh AE (2005) The application of statistical physics to evolutionary biology. *Proceedings of the National Academy of Sciences of the United States of America* 102(27):9541–9546.

[54] Kauffman S, Levin S (1987) Towards a general theory of adaptive walks on rugged landscapes. *Journal of Theoretical Biology* 128(1):11–45.

[55] Kryazhimskiy S, Tkačik G, Plotkin JB (2009) The dynamics of adaptation on correlated fitness landscapes. *Proceedings of the National Academy of Sciences* 106(44):18638–18643.

[56] Schuster P, Fontana W, Stadler PF, Hofacker IL (1994) From Sequences to Shapes and Back: A Case Study in RNA Secondary Structures. *Proceedings of the Royal Society of London B: Biological Sciences* 255(1344):279–284.

[57] Friedlander T, Mayo AE, Tlusty T, Alon U (2015) Evolution of bow-tie architectures in biology. *PLoS Comput Biol* 11(3):e1004055.

[58] Friedlander T, Prizak R, Guet CC, Barton NH, Tkačik G (2016) Intrinsic limits to gene regulation by global crosstalk. *Nature Communications* 7:12307.

[59] Shultzaberger RK, Maerkl SJ, Kirsch JF, Eisen MB (2012) Probing the Informational and Regulatory Plasticity of a Transcription Factor DNABinding Domain. *PLoS Genetics* 8(3):e1002614.

[60] Rowland MA, Deeds EJ (2014) Crosstalk and the evolution of specificity in two-component signaling. *Proceedings of the National Academy of Sciences* 111(15):5550–5555.

[61] Eldar A (2011) Social conflict drives the evolutionary divergence of quorum sensing. *Proceedings of the National Academy of Sciences* 108(33):13635–13640.

[62] Aakre C et al. (2015) Evolving New Protein-Protein Interaction Specificity through Promiscuous Intermediates. *Cell* 163(3):594–606.

[63] Sengupta AM, Djordjevic M, Shraiman BI (2002) Specificity and robustness in transcription control networks. *Proceedings of the National Academy of Sciences* 99(4):2072–2077.

[64] de Vos MGJ, Dawid A, Sunderlikova V, Tans SJ (2015) Breaking evolutionary constraint with a tradeoff ratchet. *Proceedings of the National Academy of Sciences* 112(48):14906–14911.